Astrophysics and Stellar Astronomy.
General Relativity and Gravity

UDC 551.46+53.09 https://www.doi.org/10.33910/2687-153X-2021-2-1-41-48

Tide level in time and frequency domains at Dili port: Characteristic feature of a Lorentz oscillator

A. F. Belo✉[1], K. Sasa[2], J. M. Marques[2], K. Shimakawa[3]

[1] East Timor National University, Av. Cidade de Lisboa, Díli, East Timor
[2] Dili Port Technical Authority, Edificio Central da APORTIL, Dili, East Timor
[3] Gifu University, 1–1 Yanagido, Gifu 501-1193, Japan

Authors
Abelito Filipe Belo, e-mail: abelitofilipe@gmail.com
Kenji Sasa
Jose Madeira Marques
Koichi Shimakawa

For citation: Belo, A. F., Sasa, K., Marques, J. M., Shimakawa, K. (2021) Tide level in time and frequency domains at Dili port: Characteristic feature of a Lorentz oscillator. *Physics of Complex Systems*, 2 (1), 41–48. https://www.doi.org/10.33910/2687-153X-2021-2-1-41-48

Received 18 January 2021; reviewed 28 January 2021; accepted 28 January 2021.

Abstract. Tide level during one year in time-domain measured at Dili port (East Timor) is analyzed by the frequency spectrum with the Fast Fourier Transform (FFT), together with the autocorrelation function (AF). The frequency spectrum shows a characteristic feature of the Lorentz-type resonance (Lorentz oscillator) with the special peaks which are attributed to the major tide constituents related to the gravitational motions of the sun and the moon. The Lorentz-type resonance occurs in water fluid systems under the periodic change in gravitational potential, which is similar to the electronic polarization under an electric potential change. The $1/f$ characteristics found at high frequencies in the power spectrum (the so-called $1/f$ characteristics in frequency domain) can be originated *only* from the gravitational effect, while its origin is usually discussed in terms of meteorology such as atmospheric pressure.

Keywords: tide level, fast Fourier transform (FFT), autocorrelation function, Lorentz oscillator, $1/f$ fluctuation.

Introduction

The tide level should have time-to-time variations (time domain), involving periodic cycles (Banno, Kuriyama 2012; Kleinhans et al. 2017; Pugh 1996) due to gravitational actions. Meteorological effects such as atmospheric pressure may induce a complexity in the tide level. A popular technique for analyzing tides is the harmonic analysis (HA) in time domain (TD), in which the series of N harmonic constituents (sinusoids) are assumed (Pawlowicz et al. 2002; Ro et al. 2007; Stephenson 2016). Constructing a histogram for the tide level should also be useful to know the probability density at a particular level (Murthy, Rahi 2014; Tomaselli et al. 2011). Another approach is to obtain a frequency spectrum (FS) in frequency domain (FD) (Franco 1997; Marone et al. 2013). The Fourier Transform (FT) is also a popular technique to obtain an FS (Banno, Kuriyama 2012).

In this study, we will principally discuss the FS of tide level at Dili Port (East Timor) that is located near the equator (8.55° S, 125.56° E). The study explores a minute-by-minute data from a one-year period. It should be mentioned that the studies on the tidal changes from the area near the equator are few. Here, we will only focus on gravitational effects, while the meteorological effects, in general, cannot be ignored (Andrade et al. 2018; Pugh 1996; Truccolo et al. 2006). It is shown that the tide levels are dominated

by four major gravitational constituents from the sun and the moon (M2, S2, K1, O1) and tide level dynamics is replicated well by the Lorentz-type resonance (Wooten 1972). The FS shows two principal peaks (diurnal and semidiurnal) (Ro 2007; Stewart 2008) and another constituent (one year), together with a 1/*f*-like characteristics at higher frequencies (Banno, Kuriyama 2012; Kogan 2008). It is also shown that the histogram of the tide level observed in time domain is approximated to be a Gaussian distribution function.

The autocorrelation function (AF) of the tide change clearly shows an equivalency to the Lorentz oscillator, suggesting that the tide flow resonates with the change of gravitational potentials. An analogy between the electronic polarization in microscopic media and the macroscopic tidal changes is of interest in complex systems in physics (Draper et al. 2014; Garrett, Cummins 2005). It is suggested, through this equivalency, that the 1/*f*-like nature originates only from the gravitational effect, while its origin is commonly attributed to a change in meteorology (Andrade et al. 2018).

Measurement system and analysis

Figure 1 shows the equipment instalation consisting of an ultrasonic system and a control circuit at Dili Port (Timor Leste) to which two of the authors are affiliated. This method is used to measure reflection between transmitting and receiving pulses of the ultrasonic wave. The pulses are controlled by the control circuit. The output pulse of the control circuit is converted and transferred to the Data Logger (DL). The DL performs the arithmetic processing of several signals from sensors which monitor the water level. The minute-by-minute annual data of the tide level are stored in the built-in memory and an SD card. The host device uses the RS-232C interface to communicate with the personal computer on which the "data processing software" is installed.

Fig. 1. Instalation of equipment consiting of an ultrasonic system and a control circuit at Dili Port (Timor Leste). *Fotografer: Author (Abelito Filipe Belo), 20 January 2021*

The DL-collected data are Fourier transformed (Fast Fourier Transform: FFT). The Fourier transform (FT) of a time-dependent function $f(t)$ is given by

$$F(f) = \int_{-\infty}^{\infty} f(t) e^{-i2\pi ft} dt , \quad (1)$$

where $F(f)$ is the Fourier spectrum and $|F(f)|^2$ is called the power spectrum, and f is the frequency (s^{-1}) (Kogan 2008; Papoulis 1962).

 https://www.doi.org/10.33910/2687-153X-2021-2-1-41-48

FFT is an algorithm that computes the discrete $F(f)$ (Zonst 2004). In general, a limited number (= 2^n) of discrete data, where n is an integer, is required to perform the FFT. We take the MATLAB programme that allows to remove this limitation and the minute-by-minute one-year period import data of the tide level (data number N = 544778) are Fourier transformed. The time interval of the data Δt is, therefore, given by t_p/N, where t_p is the period of measurement time. The frequency interval Δf is given as

$$\Delta f = \frac{1}{N\Delta t} \cdot \tag{2}$$

The autocorrelation function of a time-dependent series is the average measure of its time-domain properties, being average product of the signal $f(t)$ and a time-shifted version of itself, and is a function of the imposed time shift τ, i.e., $C(\tau) = \langle f(t)f(t+\tau)\rangle$ (Geng, Boufadel 2017; Kogan 2008). $C(\tau)$ is, therefore, useful for obtaining the information of the signal periodicity and its decay (loss of correlation), where τ is the correlation time. FT of $C(\tau)$ gives the power spectrum of $F(f)$, which is the well-known Wiener—Khintchine theorem (Kogan 2008):

$$\left|F\left(f\right)\right|^2 = 2\int_0^\infty \langle f\left(t\right) f\left(t+\tau\right)\rangle e^{-i2\pi f\tau} d\tau \tag{3}$$

Results and discussion

The tide level data at Dili Port (Timor Leste) were obtained for the period from May 2018 to July 2019. Note that the tide level is defined as the change from the chart datum level (CDL: minimum tide level is set to zero in one year). Figure 2 shows the measured time-dependent tide level $h(t)$ at every 1 minnute for one year. Amplitude modulation (AM)-like behavior (beat) is found, which is produced when two frequencies, f_1 and f_2, are close each other, i.e., the beat frequency is $f_1 - f_2$. The periodical time of the beat is, therefore, $1/(f_1 - f_2)$. Details on this issue with the harmonic analysis (HA) will be discussed later.

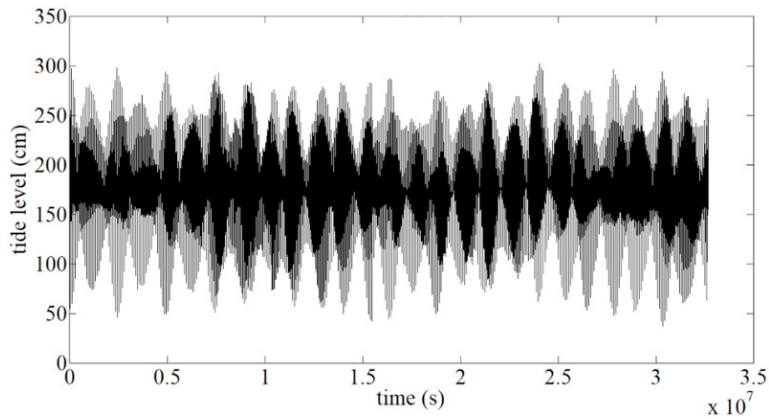

Fig. 2. Minute-by-minute one-year period data of the tide level

It may also be useful to show a histogram for the tide level h in which the probability density at a particular tide level can be obtained. The number of occurrences of each level is counted for this object. Discrete bars shown in Fig. 3 present the tide-level distribution for the total data set (N_T = 544778). It is found that the tide level follows a Gaussian distribution and is given by (Walpole et al. 2017):

$$G\left(h\right) = \frac{A}{\sqrt{2\pi\sigma^2}}\, exp\left\{-\frac{1}{2\sigma^2}\left(h-h_m\right)^2\right\}, \tag{4}$$

where A is a constant, σ is the standard deviation, and h and h_m are the tide level and its average, respectively.

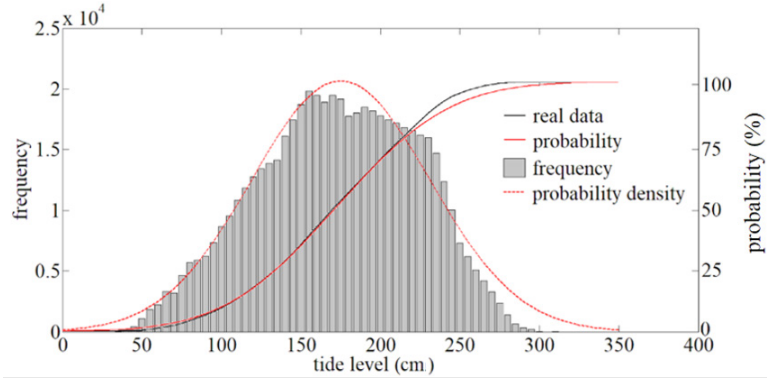

Fig. 3. Tide level distribution. Solid lines are predictions from the Gaussian (normal) distribution

The dashed line in Fig. 3 shows the probability density calculated from the $G(h)$ (A = 2.9 × 10^6, σ = 56, and h_m = 175). A more accurate comparison between the data and the probability distribution function should be given by an integral form of the histogram and the probability density, producing the probability only. Solid lines in Fig. 3 only show the probability calculated from the data (histogram) and the Gaussian distribution (red solid line) using the same parameters. Both curves fit well suggesting that the histogram basically follows a Gaussian distribution.

As is already stated, the discussion of the autocorrelation function $C(\tau)$ may be helpful to understand the underlying physics of the tide change, which produces information on the periodicity and keeps memory of the time of events (Kogan 2008). Figure 4 shows the autocorrelation functions of the practical tide for the imposed time shift, (a) τ_{max} = 30 days (2.59 × 10^6 s) and for (b) τ_{max} = one day (8.64 × 10^4 s). Here, we use the correlation time τ (not t) as a time variation. As seen for the $h(t)$ in Fig. 2, $C(\tau)$ shows the periodicity with beat. The time at which $C(\tau)$ is first crossing zero is a characteristic time τ_0 ($C(\tau_0) = 0$), which is a measure of the time of losing memory of an event and is estimated to be 1.25 × 10^4 s (~3.5 hr). The first (positive) peak at 4.54 × 10^4 s (~12.6 hr) and the second one at 8.96 × 10^4 s (~24.9 hr), respectively, are the mode frequencies of semidiurnal and diurnal changes in $h(t)$ (see also Fig. 2).

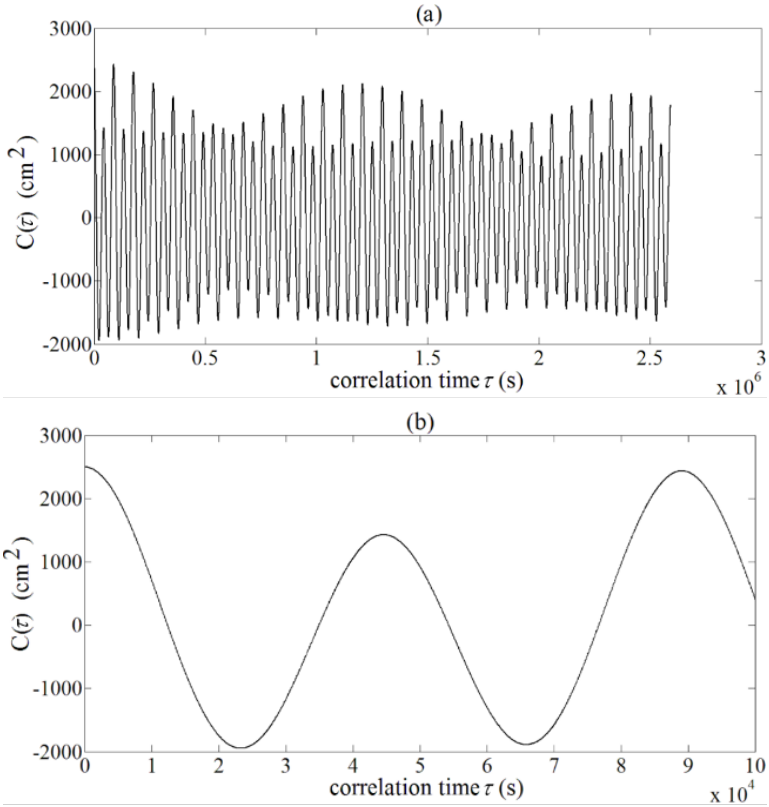

Fig. 4. Autocorrelation functions of the practical tide for (a) τ_{max} = one month, and for (b) τ_{max} = one day

 https://www.doi.org/10.33910/2687-153X-2021-2-1-41-48

These semidiurnal (M2 = 2.236 × 10^{-5} Hz, S2 = 2.315 × 10^{-5} Hz) and diurnal (K1 = 1.161 × 10^{-5} Hz, O1 = 1.076 × 10^{-5} Hz) modes can be attributed to the four major gravitational constituents from the sun and the moon. Magnitude of the semidiurnal mode is larger than the diurnal one (see Table 1).

Table 1. Standard values of relative amplitude and frequency for the semidiurnal (M2, S2) and diurnal (K1, O1) gravitational components of tide (Stewart 2008)

	Relative amplitude A_n	Frequency f_n (Hz)	Phase θ_n (rad)
M2	0.454	2.236 × 10^{-5}	–2.2
S2	0.212	2.315 × 10^{-5}	–1.6
K1	0.266	1.161 × 10^{-5}	0.0
O1	0.189	1.076 × 10^{-5}	–0.5

The beat periods related to the semidiurnal mode should be 1.27 × 10^6 s and to diurnal one, 1.18 × 10^6 s, which is consistent with the actual data shown in Fig. 2. The same beat periodicity on the $C(t)$ is found in Fig. 4 (a). The sinusoidal-like periodic response is similar to the Lorentz-type resonance in time domain, i.e.,

$$C(t) = Ae^{-\gamma t}\cos 2\pi f_0 t \ , \tag{5}$$

where A is the amplitude of displacement, γ the decay rate (s^{-1}), and f the frequency (Kogan 2008). The Lorentz-type displacement $Y(f)$ in frequency domain, i.e., the Fourier transform of $C(t)$, is known as (Kogan 2008; Wooten 1972)

$$Y(f) = \frac{B}{\left(f_0^{\,2} - f^2\right) - i\gamma f} \ , \tag{6}$$

where B is a constant, f_0 is the resonance frequency, and γ is the damping frequency (decay rate in time domain).

The solid (black) line (a) in Fig. 5 shows the power spectrum $|H(f)|^2$ ($cm^2\ Hz^{-1}$) obtained from the FFT of the time-variation of real tide $h(t)$ (practical data). The semidiurnal and diurnal peaks appear at ~2.3 × 10^{-5} Hz (peak 1) and 1.1 × 10^{-5} Hz (peak 2), respectively. Each peak splits into two peaks, producing the beats in $h(t)$ in time domain (see Fig. 2). Peaks 1 and 2, respectivey, are composed of the K_1 and O_1 and M_2 and S_2. The beats from the sets of (K_1,O_1) and (M_2 and S_2) are found in $h(t)$ shown in Fig. 2.

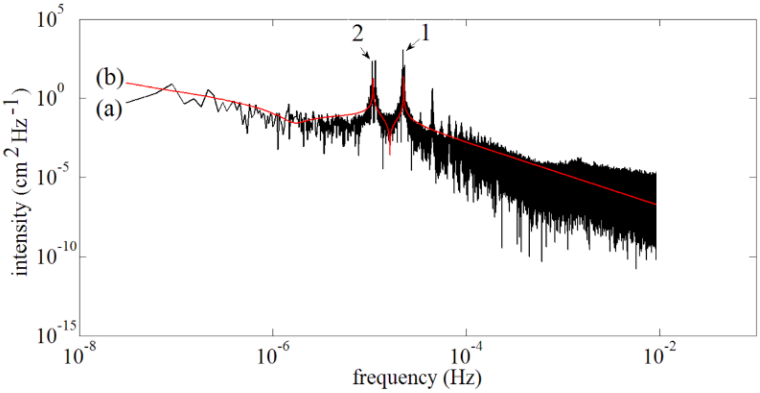

Fig. 5. Power spectrum of the tide level. Black solid line (a) is practical data; red line (b) is the model tide (Lorentz oscillators). 1 and 2 are the semidiurnal and diurnal peaks, respectively

Supposedly, the tidal change follows the Lorentz-type relaxation and the discussion in the frequency domain may clarify this point. Using eq. (5), the power spectrum $|H(f)|^2$ is approximated by|

$$\left|H(f)\right|^2 = \sum_{i=1}^{n} \frac{B_i}{\left(f_{0i}^{\,2} - f^2\right) - i\gamma_i f} \ , \tag{7}$$

where B_i is a constant, f_{0i} and γ_i is the resonant frequency and the damping frequency for i-th component, respectively. The solid line (b) shows the absolute intensity of the Lorentz oscillator (here $|H(f)|^2$) with the fitting parameters given in Table 2.

Table 2. Physical parameters for the Lorentz oscillators used for the fitting. C_i is the relative amplitude of B_i of the component (see text)

	f_{0i} (Hz)	B_i (cm² × Hz)	γ_i (Hz)	C_i
semidiurnal	2.28×10^{-5}	1.0×10^{-11}	1.0×10^{-8}	0.63
diurnal	1.10×10^{-5}	6.1×10^{-12}	1.0×10^{-8}	0.36
1 year	3.17×10^{-8}	2.0×10^{-13}	7.0×10^{-7}	0.01

For simplicity, we took one (average) frequency for the semidiurnal and dirnurnal peaks. At lower frequencies, in addition to these two peaks, we need another 3rd component (one-year periodicity) (Banno, Kuriyama 2012), since the $|H(f)|^2$ takes a constant value, without the 3rd component. Overall fitting of the Lorentz oscillator, including the 3rd constituent, to the practical data is reasonably good. At higher frequencies, we observe a decrease in the intensity with increasing frequency f, which is approximately proportional to $1/f^2$. This type of frequency-dependent behavior is similar to the $1/f$ noise or $1/f$ fluctuation (Kogan 2008). Note that the relative magnitudes of the Lorentz oscillator C_i in Table 2 are consistent with the relative intensity of the gravity constituents (M2 + S2, K1 + O1) (see Table 1).

Let us discuss tidal dynamics in more detail. It was shown that the power spectrum of the tide change was replicated well by the Lorentz oscillator. A popular example of the Lorentz oscillator (harmonic oscillation with damping) can be the dynamics of an electronic polarization, i.e., electronic displacement under a periodic electric field motion (complex dielectric function) (Wooten 1972) or a mechanical spring motion. For electronic displacement x under the external field F, the system follows Newton's second law as

$$M\frac{d^2x}{dt^2}+\gamma\frac{dx}{dt}+\omega_0{}^2x=F=Ae^{-i\omega_0 t} \quad , \tag{8}$$

where M is a mass (electronically charged), γ is the damping coefficient, and ω_0 is the angular resonant frequency (= $2\pi f_0$). The solution of the above equation under some conditions gives Eq. (5) or (6). When the second term in Eq. (8) is dominant, the Debye type dielectric relation dominates the system (no oscillation). Note also that the above resonant phenomena can be represented by an equivalent electrical circuit, i.e., *RLC* series connection (resonance circuit), where R is the resistance, L the inductance, and C the capacitance in the sense of electrical engineering (Kogan 2008; Prandle 1980). It was interesting to find out that the water fluid system under the periodic change in gravitational potential is phenomenologically the same as the electronic polarization under an electric potential change.

In addition to gravitational motion of the sun, the moon, and the earth, meteorology effects such as atmospheric pressure and wind power also contribute to the tide level (Andrade et al. 2018; Truccolo et al. 2006). Other contributing factors include the shape of the beach, coastline, and coastline depth (Kleinhans et al. 2017; Marone et al. 2013). While all these oceanic effects may dominate tidal behaviors, here we discuss the gravitational effect only. We once again suggest that the $1/f$-like nature at high frequencies originates gravitationally (nature of low-pass filter) without involving a meteorological effect.

Finally, we briefly discuss the harmonic analysis (HA) in time domain (Stewart 2008). We can model the series with I harmonic constituents of sinusoids (Stephenson 2016):

$$h(t)=H_0+C\sum_{i=1}^{I}A_n\cos\left(2\pi f_n t+\theta_n\right), \tag{9}$$

where A_n is the relative amplitude of the nth component (cm), f_n is the frequency (Hz), θ_n is the phase angle (rad), H_0 is the mean sea-level (cm) and C is the multicable constant (cm). In the present study, H_0 (= 180 cm), C (= 105 cm), and θ_n is taken as fitting parameters, while the major constituents (M2, S2, K1, O1) are taken as the tide wave of gravitational origin (I = 4) (see Table 1). Here, a one-year constituent (Matsumoto et al. 1995) was not involved in the HA. Comparisons of the actual tide change (black) with the model tide (red) are shown in Fig. 6 for the first one month. It is shown that the actual tide level is replicated well by the standard four parameters, M2, S2, K1, and O1 with some deviations.

 https://www.doi.org/10.33910/2687-153X-2021-2-1-41-48

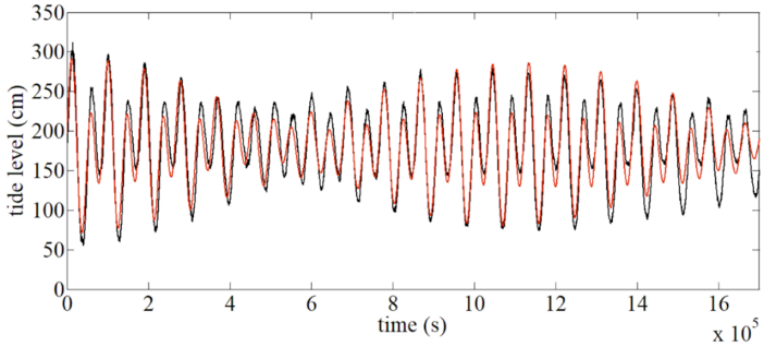

Fig. 6. Actual tide (black) and model tide (red) for the first one month

Conclusion

The minute-by-minute change in the tide level for a one-year period was measured at Dili port (East Timor). It was found that the histogram of the tide level in time-domain was approximated to be the Gaussian distribution function, with the mean height of 175 cm and the standard deviation of 56 cm. The frequency spectra through the Fast Fourier Transform (FFT) showed the two clear peaks (semidiurnal and diurnal) induced by the gravitational motions of the sun, the moon, and the earth. It was also suggested that the constituent of one-year dominated the power spectrum at low frequencies with no clear peak. The power spectrum was replicated well by the Lorentz oscillator, indicating that the tide flow resonates with the gravitational forces, which is phenomenologically the same as the electronic polarization under the electric field: *Microscopic dynamics spans to macroscopic one*. The spectrum shows the $1/f$ nature found at higher frequencies in the frequency spectra is a result of the Lorentz-type response. Origin of $1/f$ characteristics can therefore be attributed only to the gravitational effect without involving the meteorological one. It was shown by a harmonic analysis that the actual tide change was replicated well by the four standard gravitational parameters, M2, S2, K1, and O1. It was concluded that tidal behavior follows *nature's orders* even in *complex systems* of the globe.

Acknowledgments

We would like to thank Professor T. Kobayashi, Gifu University, for his useful contribution. We also wish to thank the JICA CADEFEST 2 for the financial support to the Faculty of Engineering, Universidade Nacional Timor Lorosa'e.

References

Andrade, M. M., Toldo, E. E., Nunes, J. C. R. (2018) Tidal and subtidal oscillations in a shallow water system in southern Brazil. *Brazilian Journal of Oceanography*, 66 (3), 245–254. https://doi.org/10.1590/s1679-87592018017406603 (In English)

Banno, M., Kuriyama, Y. (2012) The characteristic of shoreline response to cyclic tidal change. *Journal of Japan Society of Civil Engineers, Series B2 (Coastal Engineering)*, 68 (2), 576–580. https://www.doi.org/10.2208/kaigan.68.I_576 (In Japanese)

Draper, S., Adcock, T. A., Borthwick, A. G., Houlsby, G. T. (2014) An electrical analogy for the Pentland Firth tidal stream power resource. *Proceedings of the Royal Society A*, 470 (2161), article 20130207. https://www.doi.org/10.1098/rspa.2013.0207 (In English)

Franco, A. S. (1988) *Tides: fundamentals, analysis and prediction*. São Paulo: Fundação Centro Tecnológico de Hidráulica, 249 p. (In English)

Garrett, C., Cummins, P. (2005) The power potential of tidal currents in channels. *Proceedings of the Royal Society A: Mathematical, Physical and Engineering Sciences*, 461 (2060), 2563–2572. https://doi.org/10.1098/rspa.2005.1494 (In English)

Geng, X., Boufadel, M. C. (2017) Spectral responses of gravel beaches to tidal signals. *Scientific Reports*, 7, article 40770. https://www.doi.org/10.1038/srep40770 (In English)

Kleinhans, M. G., van der Vegt, M., Leuven, J. et al. (2017) Turning the tide: Comparison of tidal flow by periodic sea level fluctuation and by periodic bed tilting in scaled landscape experiments of estuaries. *Earth Surface Dynamics*, 5 (4), 731–756. https://www.doi.org/10.5194/esurf-5-731-2017 (In English)

Kogan, S. (2008) *Electronic noise and fluctuations in solids*. Cambridge: Cambridge University Press, 376 p. (In English)

Marone, E., Raicich, F., Mosetti, R. (2013) Harmonic tidal analysis methods on time and frequency domains: Similarities and differences for the Gulf of Trieste, Italy, and Paranaguá Bay, Brazil. *Bollettino di Geofisica Teorica ed Applicata*, 54 (2), 183–204. https://www.doi.org/10.4430/bgta0068 (In English)

Matsumoto, K., Ooe, M., Sato, T., Segawa, J. (1995) Ocean tide model obtained from TOPEX/POSEIDON altimetry data. *Journal of Geophysical Research: Oceans*, 100 (C12), 25319–25330. https://www.doi.org/10.1029/95JC02777 (In English)

Murthy, K. S. R., Rahi, O. P. (2014). Estimation of Weibull parameters using graphical method for wind energy applications. In: *2014 Eighteenth National Power Systems Conference (NPSC)*. Guwahati: IEEE Publ. [Online]. https://www.doi.org/10.1109/NPSC.2014.7103858 (accessed 10.01.2021). (In English)

Papoulis, A. (1962) *The fourier integral and its applications*. New York: McGraw-Hill Publ., 318 p. (In English)

Pawlowicz, R., Beardsley, B., Lentz, S. (2002) Classical tidal harmonic analysis including error estimates in MATLAB using T_TIDE. *Computers & Geosciences*, 28 (8), 929–937. https://www.doi.org/10.1016/S0098-3004(02)00013-4 (In English)

Prandle, D. (1980) Modelling of tidal barrier schemes: An analysis of the open-boundary problem by reference to AC circuit theory. *Estuarine and Coastal Marine Science*, 11 (1), 53–71. https://www.doi.org/10.1016/S0302-3524(80)80029-6 (In English)

Pugh, D. T. (1996) *Tides, surges and mean sea-level: A handbook for engineers and scientists*. Chichester: Wiley Publ., 472 p. (In English)

Ro, Y. J. (2007) Tidal and sub-tidal current characteristics in the Kangjin Bay, South Sea, Korea. *Ocean Science Journal*, 42 (1), 19–30. https://www.doi.org/10.1007/BF03020907 (In English)

Ro, Y. J., Jung, K. Y., Jun, W. S., Eom, H. M. (2007) Numerical modeling of tide and tidal current in the Kangjin Bay, South Sea, Korea. *Ocean Science Journal*, 42 (3), 153–163. https://www.doi.org/10.1007/BF03020919 (In English)

Stephenson, A. G. (2016) *TideHarmonics: Harmonic analysis of tides*. [Online]. Available at: https://cran.r-project.org/package=TideHarmonics (accessed 10.01.2021). (In English)

Stewart, R. H. (2008) *Introduction to physical oceanography*. [Online]. Available at: http://hdl.handle.net/1969.1/160216 (accessed 10.01.2021). (In English)

Tomaselli, P. D., Re, C. L., Ferreri, G. B. (2011) Analysis of tide measurements in a Sicilian harbour. In: H. Schüttrumpf, R. Tomasicchio (eds.). *5th SCACR 2011. International Short Conference on Applied Coastal Research*. Graz: Institute of Hydraulic Engineering and Water Resources Management Publ., pp. 579–586. (In English)

Truccolo, E. C., Franco, D., Schettini, C. A. F. (2006) The low frequency sea level oscillations in the northern coast of Santa Catarina, Brazil. *Journal of Coastal Research*, SI 39, 547–552. (In English)

Walpole, R. E., Myers, R. H., Myers, S. L., Ye, K. (2017) *Probability and statistics for engineers and scientists*. 9th ed. Singapore: Pearson Education South Asia Pte Ltd. Publ., 811 p. (In English)

Wooten, F. (1972) *Optical properties of solids*. New York: Academic Press, 272 p. https://doi.org/10.1016/C2013-0-07656-6 (In English)

Zonst, A. E. (2004) *Understanding the FFT applications: A tutorial for students & working engineers*. 2nd ed., rev. Titusville: Citrus Press., 182 p. (In English)